Applied Surface Science 445 (2018) 563–567

Contents lists available at ScienceDirect

Applied Surface Science

journal homepage: www.elsevier.com/locate/apsusc

Full Length Article

Layer thickness effect on fracture behavior of Al/Si_3N_4 multilayer on Si substrate under three-point bending

M. Wang [a,*], D. Wang [b], P. Schaaf [b]

[a] School of Materials Science and Engineering, Liaoning Technical University, Zhonghua Road 47, 123000 Fuxin, China
[b] Materials for Electronics, Institute of Materials Engineering and Institute of Micro-and Nanotechnologies MacroNano®, TU Ilmenau, Gustav-Kirchhoff-Str. 5, 98693 Ilmenau, Germany

ARTICLE INFO

Article history:
Received 14 September 2017
Revised 1 February 2018
Accepted 22 February 2018
Available online 24 February 2018

Keywords:
Layer thickness effect
Three-point bending
Metallic/ceramic multilayers
Fracture behavior
Fracture mechanism

ABSTRACT

The fracture behavior of multilayers in the nanometer thickness range has attracted an increased attention due to microelectronics and high-speed technologies. In this work, Al/Si_3N_4 multilayers fabricated by magnetron sputtering on the silicon substrate were subjected to three-point bend testing. It was investigated that the fracture behavior of Al/Si_3N_4 multilayers with different individual layer thickness λ (50, 100, 250 nm) but with the same total thickness (1.0 μm). There is a significant layer thickness effect on the fracture behavior of the whole multilayer-substrate system: when the individual layer thickness is large (250 nm), the failure of the whole system was dominated by the fracture of the substrate, while the failure of the whole system was dominated by the fracture of the multilayer with smaller individual layer thickness (50 nm). This effect is clearly obvious, although the total thickness of the multilayer is very small compared with that of the substrate. As the individual layer thickness decreased from 250 nm to 50 nm, the fracture strain on the Al/Si_3N_4 multilayer decreased from 0.073% to 0.026%.

1. Introduction

Nano-multilayered composites have attracted an increased research attention for more than a decade [1–6] due to the distinct electrical [7–9], magnetic [10], optical [11,12] and mechanical properties [13–16]. Increasing interest is also paid on the investigation of deformation and fracture behaviors of the multilayered composites due to the implication on the reliability issue in the applications.

For metal film on the flexible substrate, experimental testing results have shown that most flexible-supported thin metal films rupture at small tensile strain [17–25]. However, theoretical calculations showed that delocalizing strain of the polymer substrate caused the metal film elongating indefinitely [26,27]. This difference between experiment and theory may be caused by the effects of very small grain size, thin film thickness and inadequate interfacial adhesion [22,27].

It was studied that there exists a significant length-scale or layer thickness effect on the deformation behavior and the strength of metallic/ceramic multilayers on the brittle substrate. When the individual layer thickness decreased to sub-micron scale or even nanometer scale, where the thinner the individual layer is, the higher the strength is [28–37]. It was further reported that the deformation of the multilayers with sub-micron layer thicknesses is dominated by the pileup of dislocations at interfaces, and the increase in strength follows a Hall-Petch relationship with $\sigma_{flow} \propto \lambda^{-0.5}$, where λ is the individual layer thickness [34,38–40]. However, when the layer thickness is further decreased to the range of 10–50 nm, there is no enough space to accommodate dislocation pileup in the individual layers, and the deformation mechanism is dominated by Orowan-type bowing of individual dislocations and the increase of strength follows with $\sigma_{flow} \propto \ln(\lambda/b)/\lambda$ [14,34].

There are, however, only a few systematic studies on the layer thickness effect on the fracture behavior of metal/ceramic multilayers systems [41–47]. In most of these papers, a systematic study of the variation of fracture behaviors with layer thickness was presented, including Al/SiN/GaAs multilayers [41], Ti/ZrO_2 multilayers [42], Ti/TiN multilayers [28], Cr/CrN multilayers [45], Ti/TiAlSiN multilayers [46] and V/NiAl multilayers [47], but the dependence of fracture behavior on the layer thickness is still almost unexplored. Most of previous studies focused on the fracture behaviors of metallic/ceramic multilayers under nanoindentation. Different loading way was corresponding to different stress situation, which caused different fracture behaviors for the same multilayered film. However, there was the lack of the layer thickness effect on the fracture behaviors of the whole multilayer-substrate system under

* Corresponding author.
E-mail address: mwang.lntu@hotmail.com (M. Wang).

https://doi.org/10.1016/j.apsusc.2018.02.223
0169-4332/

three-point bending. In this paper, individual-layer-thickness effect on fracture behavior of Al/Si_3N_4 multilayers on Si substrate under three-point bending is investigated and discussed. It is found that not only the fracture behavior of the multilayer itself, but also the fracture behavior of the whole multilayer-substrate system is clearly dependent on the individual layer thickness. When the individual layer thickness is large (250 nm), the failure of the whole system was dominated by the fracture of the substrate, while the failure of the whole system was dominated by the fracture of the multilayer with smaller individual layer thickness (50 nm).

2. Experimental

Al/Si_3N_4 multilayer films were deposited on (1 0 0) oriented 393 μm-thick Si wafers using DC and RF magnetron sputtering at a base pressure of 5.0×10^{-5} Pa with a power of 210 W and 110 W, respectively. Before deposition, the Si wafers were cleaned with 7% HF acid. The deposition rate was 1.56 nm/s for Al and 0.18 nm/s for Si_3N_4. The individual layer thickness λ was identical for Al and Si_3N_4 layers, and 3 types of multilayers were fabricated with different individual layer thicknesses of 50 nm, 100 nm and 250 nm. The total thickness of the multilayer films was always 1.0 μm and the surface layer (topmost layer) was always Al.

The X-ray diffraction (XRD) experiment was carried out in Bragg-Brentano geometry with Cu Kα radiation (Siemens D5000). The TEM lamellar samples before the bending test were prepared with focused ion beam microscope (FIB, Zeiss nanoanalytics Auriga 60). The original cross-sectional microstructure of the multilayers was observed by transmission electron microscope (TEM, FEI Tecnai 20S-TWIN). The fracture behaviors of the multilayers with different individual thicknesses were investigated by three-point bending test with the loading rate 1.0 μm/s, as shown in Fig. 1. The bending test of the multilayers was applied for five times corresponding to every individual layer thickness. The length, the width and the span (L_s) of the bending specimen was 90, 10 and 70 mm, respectively. The fracture behavior was investigated by using a field-emission scanning electron microscope (SEM, Hitachi S 4800).

3. Results and discussion

Fig. 2 shows the XRD patterns of the multilayers with different individual layer thickness. The (1 1 1) diffraction peaks of Al were observed for all the Al/Si_3N_4 multilayers with different individual thickness, while the (2 0 0), (2 2 0) and (3 1 1) diffraction peaks of Al were only observed for the 100 nm-thick Al layers and 250 nm-thick layers. This indicates that the (1 1 1) out-of-plane texture became stronger with decreasing the individual layer thickness. There were no diffraction peaks observed corresponding to the peaks of crystalline Si_3N_4, indicating that the Si_3N_4 layers are

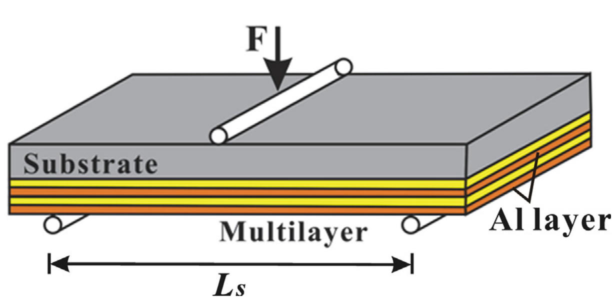

Fig. 1. Schematic diagram of macroscopic structure of Al/Si_3N_4 multilayers on Si (1 0 0) substrates under three-point bending test.

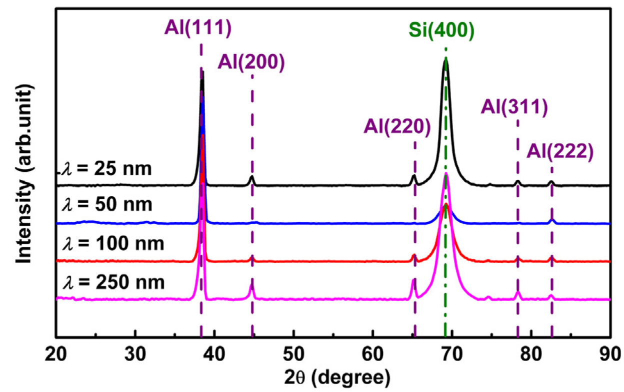

Fig. 2. X-ray diffraction patterns of Al/Si_3N_4 multilayers with different individual thicknesses.

amorphous. In order to clarify the microstructure of the multilayers with different individual thicknesses, the TEM investigation has been performed and the TEM cross-sectional morphology of the multilayers is shown in Fig. 3. Columnar grain structure was found both in the 50 nm-thick Al layers (Fig. 3(a)) and in the 250 nm-thick Al layers (Fig. 3(b)).

Fig. 4(a) shows the relationship between the loading force and the bending deflection for the whole multilayer-substrate system with different individual layer thicknesses. From Fig. 4(a) it can be found that the deflection at fracture became higher as the individual layer thickness increased. Moreover, the deflection at fracture of the 250 nm-thick multilayer was similar with that of the Si substrate. The whole Al/Si_3N_4 multilayer subjected to the tensile stress during the three-point bending test, because the total thickness of the Al/Si_3N_4 multilayer (1.0 μm) was far less than the thickness of the Si substrate (393 μm). Generally, the bending strain on the multilayers can be evaluated by Eq. (1), which is as follows:

$$\varepsilon_{\text{top}} = \frac{M_{\max} \cdot (h_m + h_s)}{2EI_z} \cdot \frac{1 + 2\beta + \alpha\beta^2}{(1 + \beta) \cdot (1 + \alpha\beta)} \tag{1}$$

in which, $M_{\max} = \frac{FL_s}{4}$, $F = \frac{48EI_z f_c}{L_s^3}$, $\alpha = \frac{E_m}{E_s}$, $\beta = \frac{h_m}{h_s}$. M_{max} is the max bending moment; I_z is the moment of inertia of the cross section for the neutral plane; EI_z stands for the bending stiffness of the whole specimen; L_s is the span of the specimen; E_m and E_s is the elastic modulus of the multilayer and the substrate, respectively; h_m and h_s is the thickness of the multilayer and the substrate; f_c is the deflection of the multilayers. Due to $\beta \ll 1$, the bending strain can be described by Eq. (2) as follows:

$$\varepsilon_{\text{top}} = \frac{6(h_m + h_s) \cdot f_c}{L_s^2} \tag{2}$$

According to the Eq. (2), the bending strain of the multilayers at fracture was obtained with different individual layer thickness as shown in Fig. 4(b). From Fig. 4(b) one can see that the bending strain of the multilayers at fracture increases with the individual layer thickness increasing, indicating the size effect on the bending deformation ability of the Al/Si_3N_4 multilayers. The thicker the individual layer is, the higher the bending deformation ability is. Moreover, in this work, because the Al/Si_3N_4 multilayers were sputtered on the Si substrate, the multilayers and Si substrate were subjected to the bending deformation together during the three-point bending test. Therefore, the multilayers were confined by the Si substrate in the bending process. The surface strain of Si substrate at fracture was far higher than that of the 50 nm-thick multilayer at fracture. This indicated that the fracture of the multilayers is extended in the whole multilayer-substrate system.

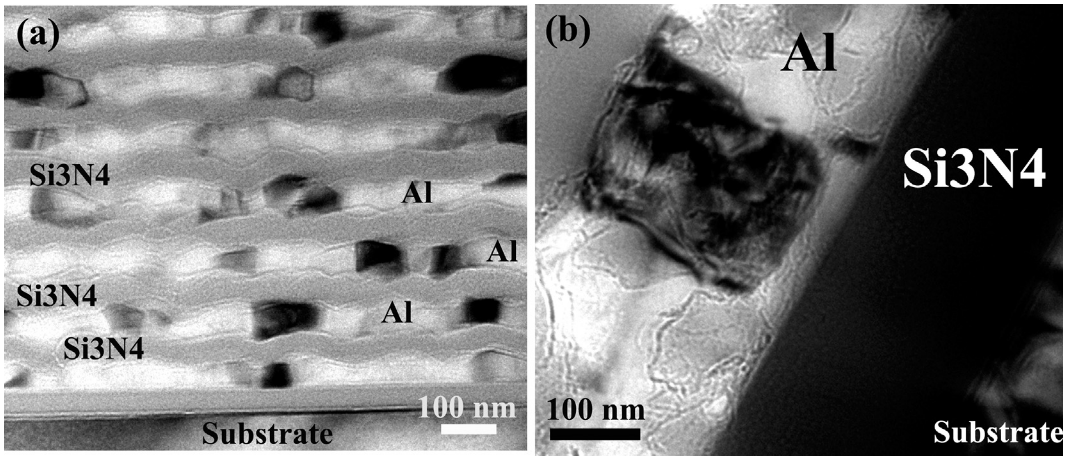

Fig. 3. TEM cross sectional images of Al/Si_3N_4 multilayers with individual layer thicknesses of 50 nm (a) and 250 nm (b).

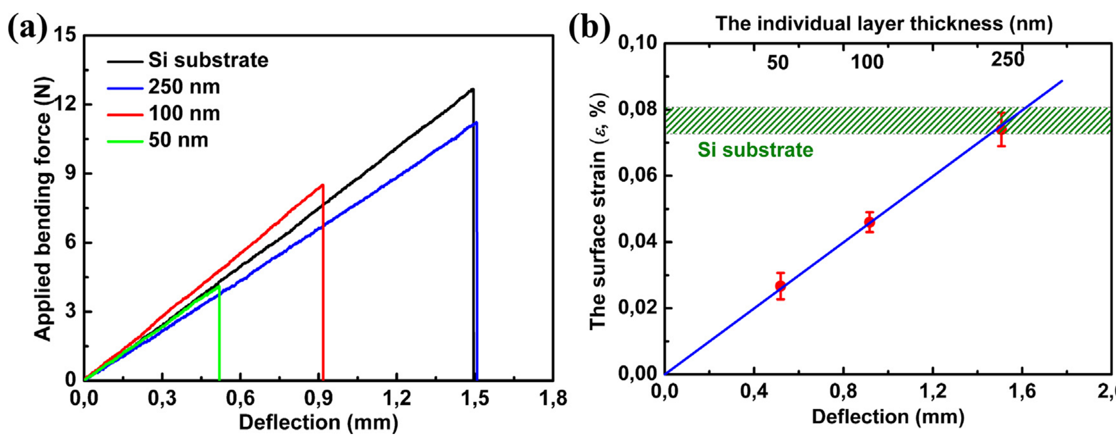

Fig. 4. (a) The relationship between applied load and the bending deflection of the Si substrate and the Al/Si_3N_4 multilayers with different individual layer. (b) Variation of the bending strain with the bending deflection obtained from different layer-thick multilayer at fracture.

As the individual layer thickness increased from 50 nm to 100 nm, the fracture is still over the whole system. With the individual layer thickness increasing to 250 nm, the surface strain of the multilayer at fracture was comparative with that of the Si substrate. This caused the fracture in the Si substrate more pronounced.

Fig. 5 shows the fracture morphology of Al/Si_3N_4 multilayers with different individual layer thickness. The insets in Fig. 5(a), (c) and (e) show the macroscopic fracture morphology corresponding to the different individual layer thickness, respectively. Fig. 5 (b), (d) and (f) is the magnified view of the rectangle region in Fig. 5(a), (c) and (e), respectively. Al layers was marked by the arrow in Fig. 5(b), (d) and (f). From the insets with different individual layer thickness, it was found that the more and more broken fragments appeared with increasing the individual layer thickness. In order to clarify the fracture behaviors of the whole system between the multilayer and the substrate, the magnified observation of the multilayers was obtained as shown in Fig. 5(b), (d) and (f). It was found that the occurrence of necking in Al layers and brittle fracture in Si_3N_4 layers for 250 nm-thick multilayers (see Fig. 5(f)). Under the bending force, the multilayers can be deformed with the substrate together due to the certain plastic deformation ability. When the bending strain on the multilayers reached 0.073%, the occurrence of fracture in the substrate dominated the failure of the whole system. This is the main reason why the bending deflection of the multilayers with 250 nm layer thickness was comparative that of Si substrate (see Fig. 4(a)). With the individual layer thickness decreasing to 100 nm, there appeared the fracture stage between Al layers and Si_3N_4 layer besides the necking in Al layers and brittle fracture in Si_3N_4 layers (see Fig. 5(d)). With the bending force increasing, the tensile strain of the multilayers increased, and then the occurrence of the plastic deformation in the Al layers and the brittle fracture in the Si_3N_4 layers leaded to the delamination at interface, which caused the fracture of 100 nm-thick multilayers and then dominated the failure of the whole system, which is the main reason why the bending deflection of 100 nm-thick multilayers was less than that of Si substrate (see Fig. 4(a)). As the individual layer thickness decreased to 50 nm, which there was not distinguishing necking phenomenon in Al layers compared with the 250 nm-thick multilayers (see Fig. 5(b)). When the tensile strain of the multilayer reached 0.026% (see Fig. 4(b)), the Si substrate was not fractured (see Fig. 4(a)). However, because the plastic deformation in the metallic layer became more difficult at nanometer scale, the ability of bending deformation became lower, which caused that the multilayers fractured. This leaded to the failure of the whole system.

As above, for the Al/Si_3N_4 multilayers with layer thickness at submicron scale, it is difficult for the stress concentration formation at interface between the multilayer and the substrate, which the failure of the whole system was dominated by the fracture of substrate. For the Al/Si_3N_4 multilayers with layer thickness at nanometer scale, due to lower plastic deformation ability it is easy for the stress concentration formation at interface between the

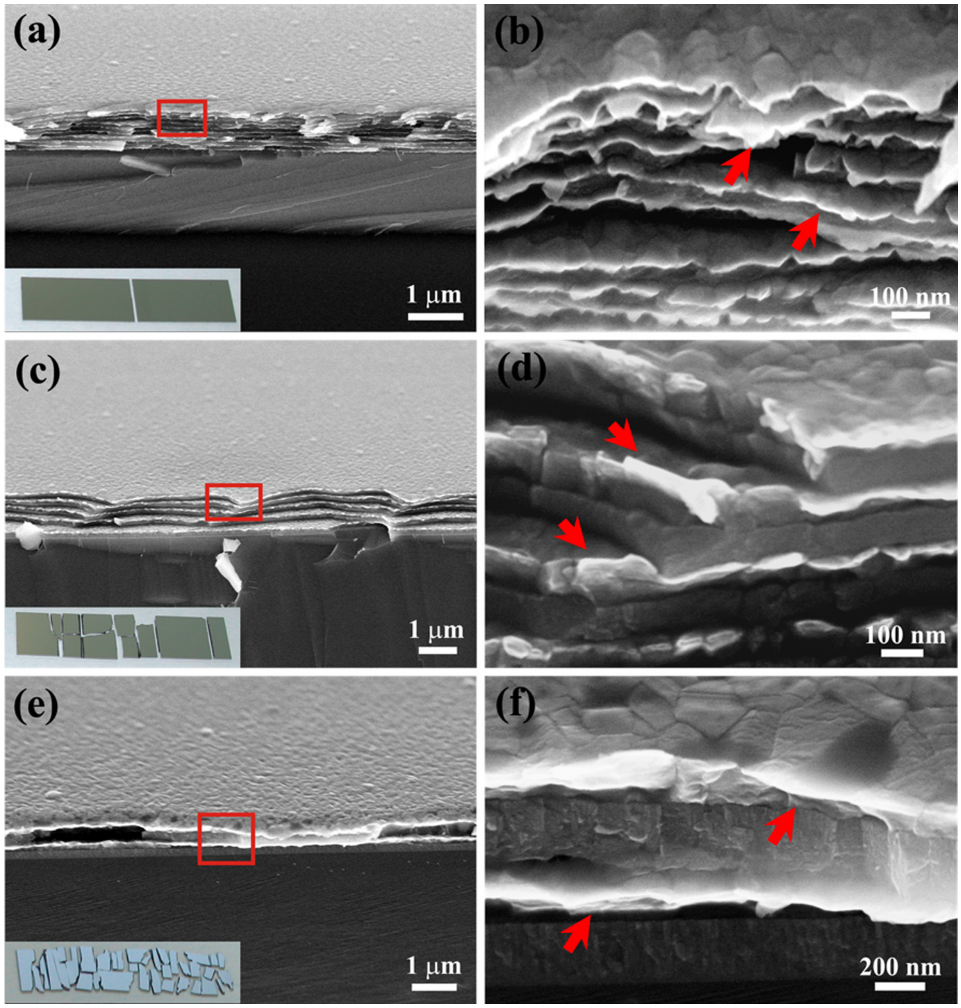

Fig. 5. SEM images of the fracture morphology around the with different individual layer-thick Al/Si_3N_4 multilayers: (a) 50 nm; (c) 100 nm; (e) 250 nm. (b), (d) and (f) corresponding to the local magnification of the rectangle region in (a), (c) and (e), respectively. Al layers were marked by the arrow. The insets in (a), (c) and (e) are the photographs of the fractured specimens.

multilayer and the substrate [34], and the failure of the whole system was dominated by the fracture of the multilayer, although the thickness of the multilayer was negligible compared with the whole film-substrate system. This explained why the broken fragments became less with the individual layer thickness decreasing from 250 nm to 50 nm.

4. Conclusion

The fracture behavior of Al/Si_3N_4 multilayers prepared on Si substrate by magnetron sputtering with different individual layer thickness was investigated under three-point bending test. There is a significant layer thickness effect on the fracture behavior of the whole multilayer-substrate system. The failure of the whole system was dominated by the fracture of substrate when the layer thickness is at submicron scale, while the failure of the whole system was dominated by the fracture of the multilayer when the layer thickness is at nanometer scale. With decreasing individual layer thickness from 250 nm to 50 nm, the fracture strain on the Al/Si_3N_4 multilayer decreased from 0.073% to 0.026%.

Acknowledgements

The authors are grateful to Rolf Grieseler and Thomas Kups for the specimen fabrication and TEM characterization. This work was supported by Liaoning Province Natural Science Foundation (20180510034), Science Research Project of Liaoning Province Education Department (L2015219) and a Postdoc fellowship of the Carl Zeiss Stiftung (Germany).

References

[1] G. Decher, J.B. Schlenoff, Functional layer-by-layer assemblies with photo- and electrochemical response and selective transport of small molecules and ions, in: Multilayer Thin Films: Sequential Assembly of Nanocomposite Materials, Wiley-VCH Verlag GmbH & Co. KGaA, Weinheim, 2003, pp. 427–460.
[2] A.K. Petford-Long, A.N. Chiaramonti, Transmission electron microscopy of multilayer thin films, Annu. Rev. Mater. Res. 38 (2008) 559–584.
[3] M.P. Soriaga, J. Stickney, L.A. Bottomley, Y.G. Kim (Eds.), Thin Films: Preparation, Characterization, Applications, Springer, US, 2002, p. 367.
[4] M. Nastazi, D. Parkin, H. Gleiter, Mechanical Properties and Deformation Behavior of Materials Having Ultra-Fine Microstructures, Springer, US, 1993, p. 624.
[5] J. Das, W. Loser, U. Kuhn, J. Eckert, S.K. Roy, L. Schultz, High-strength Zr-Nb-(Cu, Ni, Al) composites with enhanced plasticity, Appl. Phys. Lett. 82 (2003) 4690–4692.
[6] L. Thilly, P.O. Renault, V. Vidal, F. Lecouturier, S. Van Petegem, U. Stuhr, H. Van Swygenhoven, Plasticity of multiscale nanofilamentary Cu/Nb composite wires during in situ neutron diffraction: code formation and size effect, Appl. Phys. Lett. 88 (2006) 191906.
[7] T.Z. Lu, M. Alexe, R. Scholz, V. Talelaev, M. Zacharias, Multilevel charge storage in silicon nanocrystal multilayers, Appl. Phys. Lett. 87 (2005) 202110.
[8] A.L. Lima, X. Zhang, A. Misra, C.H. Booth, E.D. Bauer, M.F. Hundley, Length scale effects on the electronic transport properties of cu/nb bilayers, Thin Solid Films 515 (2007) 3574–3579.

[9] M. Wang, B. Zhang, Q.Y. Yu, C.S. Liu, G.P. Zhang, Effects of interface and grain boundary on the electrical resistivity of Cu/Ta multilayers, J. Mater. Sci. Technol. 25 (2009) 699–702.
[10] M. Albrecht, G. Hu, I.L. Guhr, T.C. Ulbrich, J. Boneberg, P. Leiderer, et al., Magnetic multilayers on nanospheres, Nat. Mater. 4 (2005) 203–206.
[11] X. Wang, H. Masumoto, Y. Someno, T. Hirai, Helicon plasma deposition of a TiO_2/SiO_2 multilayer optical filter with graded refractive index profiles, Appl. Phys. Lett. 72 (1998) 3264–3266.
[12] J. Hiltunen, D. Seneviratne, R. Sun, M. Stolfi, H.L. Tuller, J. Lappalainen, et al., $BaTiO_3$–$SrTiO_3$ multilayer thin film electro-optic waveguide modulator, Appl. Phys. Lett. 89 (2006) 1005.
[13] S.P. Dey, S.C. Deevi, Single layer and multilayer wear resistant coatings of (Ti, Al)N: a review, Mater. Sci. Eng., A 342 (2003) 58–79.
[14] A. Misra, J.P. Hirth, R.G. Hoagland, Length-scale-dependent deformation mechanisms in incoherent metallic multilayered composites, Acta Mater. 53 (2005) 4817–4824.
[15] Y.C. Wang, A. Misra, R.G. Hoagland, Fatigue properties of nanoscale Cu/Nb multilayers, Scr. Mater. 54 (2006) 1593–1598.
[16] M. Wang, D. Wang, M. Hopfeld, R. Grieseler, D. Rossberg, P. Schaaf, Nanoindentation of nano-Al/Si_3N_4, multilayers with Vickers and Brinell indenters, J. Eur. Ceram. Soc. 33 (2013) 2355–2358.
[17] O. Kraft, M. Hommel, E. Arzt, X-ray diffraction as a tool to study the mechanical behaviour of thin films, Mater. Sci. Eng., A 288 (2000) 209–216.
[18] M. Hommel, O. Kraft, Deformation behavior of thin copper films on deformable substrates, Acta Mater. 49 (2001) 3935–3947.
[19] B.E. Alaca, M.T.A. Saif, H. Sehitoglu, On the interface debond at the edge of a thin film on a thick substrate, Acta Mater. 50 (2002) 1197–1209.
[20] D.Y.W. Yu, F. Spaepen, The yield strength of thin copper films on Kapton, J. Appl. Phys. 95 (2004) 2991–2997.
[21] S.P. Lacour, S. Wagner, Z. Huang, Z. Suo, Stretchable gold conductors on elastomeric substrates, Appl. Phys. Lett. 82 (2003) 2404–2406.
[22] Y. Xiang, T. Li, Z. Suo, J. Vlassak, High ductility of a metal film adherent on a polymer substrate, Appl. Phys. Lett. 87 (2005) 161910.
[23] R.M. Niu, G. Liu, C. Wang, G. Zhang, X.D. Ding, J. Sun, Thickness dependent critical strain in submicron Cu films adherent to polymer substrate, Appl. Phys. Lett. 90 (2007) 161907.
[24] S. Frank, P. Gruber, U.A. Handge, R. Spolenak, In situ studies on the cohesive properties of α- and β-Ta layers on polyimide substrates, Acta Mater. 59 (2011) 5881–5892.
[25] M. Wang, D. Wang, P. Schaaf, Size effect on the mechanical behavior of Al/Si multilayers deposited on Kapton substrate, J. Mater. Sci.: Mater. Electron. 26 (2015) 8224–8228.
[26] T. Li, Z.Y. Huang, Z.C. Xi, S.P. Lacour, S. Wagner, Z. Suo, Delocalizing strain in a thin metal film on a polymer substrate, Mech. Mater. 37 (2005) 261–273.
[27] T. Li, Z. Suo, J. Int, Ductility of thin metal films on polymer substrates modulated by interfacial adhesion, Int. J. Solids Struct. 44 (2007) 1696–1705.
[28] B.M. Clemens, H. Kung, S.A. Barnett, Structure and strength of multilayers, MRS Bull. 24 (1999) 20–26.
[29] G. Abadias, S. Dub, R. Shmegera, Nanoindentation hardness and structure of ion beam sputtered TiN, W and TiN/W multilayer hard coatings, Surf. Coat. Technol. 200 (2006) 6538–6543.
[30] A.T. Alpas, J.D. Embury, D.A. Hardwick, R.W. Springer, The mechanical properties of laminated microscale composites of Al/Al_2O_3, J. Mater. Sci. 25 (1990) 1603–1609.
[31] M.A. Phillips, B.M. Clemens, W.D. Nix, Microstructure and nanoindentation hardness of Al/Al_3Sc multilayers, Acta Mater. 51 (2003) 3171–3184.
[32] M.A. Phillips, B.M. Clemens, W.D. Nix, Mechanical properties of Al/Al_3Sc metallic multilayers-deformation mechanisms at the nanoscale, Mater. Sci. Forum 426–432 (2003) 3373.
[33] D. Bhattacharyya, N.A. Mara, R.G. Hoagland, A. Misra, Tensile behavior of 40 nm Cu/Nb nanoscale multilayers, Scr. Mater. 58 (2008) 874–877.
[34] M. Wang, D. Wang, T. Kups, P. Schaaf, Size effect on mechanical behavior of Al/Si_3N_4, multilayers by nanoindentation, Mater. Sci. Eng., A 644 (2015) 275–283.
[35] D. Wang, T. Kups, J. Schawohl, P. Schaaf, Deformation behavior of Au/Ti multilayers under indentation, J. Mater. Sci.: Mater. Electron. 23 (2012) 1077–1082.
[36] X. Deng, N. Chawla, K.K. Chawla, M. Koopman, J.P. Chu, Mechanical behavior of multilayered nanoscale metal-ceramic composites, Adv. Eng. Mater. 7 (2010) 1099–1108.
[37] X. Deng, C. Cleveland, N. Chawla, T. Karcher, M. Koopman, K.K. Chawla, Nanoindentation behavior of nanolayered metal-ceramic composites, J. Mater. Eng. Perform. 14 (2005) 417–423.
[38] A. Misra, M. Verdier, Y.C. Lu, H. Kung, T.E. Mitchell, M. Nastasi, J.D. Embury, Structure and mechanical properties of Cu-X (X = Nb, Cr, Ni) nanolayered composites, Scr. Mater. 39 (1998) 555–560.
[39] H.B. Huang, F. Spaepen, Tensile testing of free-standing Cu, Ag and Al thin films and Ag/Cu multilayers, Acta Mater. 48 (2000) 3261–3269.
[40] L.H. Friedman, D.C. Chrzan, Scaling theory of the Hall-Petch relation for multilayers, Phys. Rev. Lett. 81 (1998) 2715–2718.
[41] J.L. Mead, M.Y. Lu, H. Huang, Inducing stable interfacial delamination in a multilayer system by four-point bending of microbridges, Surf. Coat. Technol. 320 (2017) 478–482.
[42] A. Kelling, K.R. Mangipudi, I. Knorr, T. Liese, H.U. Krebs, A. Cynthia, Volkert, Investigating fracture of nanoscale metal–ceramic multilayers in the transmission electron microscope, Scr. Mater. 115 (2016) 42–45.
[43] J.J. Roa, R. Rodríguez, V. Lamelas, R. Martínez, E. Jiménez-Piqué, L. Llanes, Small scale fracture behaviour of multilayer TiN/CrN systems: assessment of bilayer thickness effects by means of ex-situ tests on FIB-milled micro-cantilevers, Surf. Coat. Technol. 308 (2016) 414–417.
[44] M. Gruber, P. Supancic, F. Aldrian, R. Bermejo, Effect of metallization on the strength and fracture behaviour of functional co-fired multilayer ceramics, J. Eur. Ceram. Soc. 37 (2017) 4389–4396.
[45] R. Daniel, M. Meindlhumer, J. Zalesak, B. Sartory, A. Zeilinger, C. Mitterer, J. Keckes, Fracture toughness enhancement of brittle nanostructured materials by spatial heterogeneity: a micromechanical proof for CrN/Cr and TiN/SiOx multilayers, Mater. Des. 104 (2016) 227–234.
[46] A. Azizpour, E. Poursaeidi, Fracture and deformation mechanism of Ti(C, N)/TiAlSiN multilayer coating: FE modeling and experiments, Ceram. Int. 43 (2017) 1830–1838.
[47] M. Li, R. Wang, N. Katsube, W.O. Soboyejo, An investigation of the effects of layer thickness on the fracture behavior of layered NiAI/V composites, J. Eng. Mater. Technol. 121 (1999) 453.